

# Excitation and Entanglement Transfer Near Quantum Critical Points

Michael J. Hartmann,\* Moritz E. Reuter, and Martin B. Plenio

*Institute for Mathematical Sciences,  
Imperial College London, SW7 2PE, United Kingdom and  
QOLS, The Blackett Laboratory, Imperial College London,  
Prince Consort Road, SW7 2BW, United Kingdom*

(Dated: October 2, 2018)

## Abstract

Recently, there has been growing interest in employing condensed matter systems such as quantum spin or harmonic chains as quantum channels for short distance communication. Many properties of such chains are determined by the spectral gap between their ground and excited states. In particular this gap vanishes at critical points of quantum phase transitions. In this article we study the relation between the transfer speed and quality of such a system and the size of its spectral gap. We find that the transfer is almost perfect but slow for large spectral gaps and fast but rather inefficient for small gaps.

PACS numbers:

---

\*Electronic address: m.hartmann@imperial.ac.uk

## I. INTRODUCTION

Quantum Information and Condensed Matter Physics are currently two areas of very active research where several links between the two branches have been discovered in recent years. In particular, the relation of entanglement properties to critical points of quantum phase transitions has been studied in some detail. In analogy to classical phase transitions, the latter are typically characterized in terms of the scaling behavior of equilibrium properties, such as the correlation length. Analogous scaling phenomena have now been found for the entanglement properties of a spin chain in the vicinity of a critical point. [6, 7, 8, 9].

In Quantum Communication, condensed matter systems have recently received some attention as interesting candidates for quantum channels [1, 2]. This approach may be of advantage in situations where photonic quantum communication is not possible for example because the two units are only separated by a few optical wavelengths or are inside a material that does not permit for the well-controlled propagation of light.

The quantum mechanical properties of correlated many body system are to some extent determined by the energetic gap between their ground states and the lowest excited states. In particular the system is short range correlated if it features a finite gap, while some quantities can become long range correlated when the gap closes [3, 4]. The latter happens at the critical points of quantum phase transitions [5].

Motivated by these findings the dynamical entanglement properties of quantum many body systems undergoing a quantum phase transition are receiving increasing attention [10, 11, 12, 13].

To pursue the analysis of quantum many body systems as possible quantum channels a step further, we study here the connection between the spectral gap and the systems ability to transfer excitations and entanglement. However, our aim is twofold: Besides being interested in the systems transfer capacity, we also want to explore, to what degree the transfer properties can be employed to detect and characterize critical points of quantum phase transitions.

In particular, we consider spin chains and harmonic chains, where in both cases, two ancillas couple weakly to the chain at distant sites. We study the transfer of quantum information and excitations from one ancilla to the other numerically, by employing newly developed matrix product state techniques [14], and analytically with a master equation

approach. The numerics is applied to the spin chains while the master equation is used to describe the case of an harmonic chain, where its validity is confirmed numerically for Gaussian initial states [2].

Both systems show a very similar behavior: The transfer properties sensitively depend on the energy gap between the ground state and the lowest excited states, but do not significantly dependent on the detailed structure of the Hamiltonian. The quality and speed of state transfer through such systems may thus be used to detect critical points experimentally.

This paper is organized as follows: Section II begins with a discussion of spin chains, mainly employing numerical methods. In Section III a simplified picture unraveling the origin of the observed behavior is presented. This picture is then further corroborated in Section IV where we study harmonic chains both numerically and analytically with a master equation approach. Section V discusses connection to quantum channel capacities and Section VI summarizes our results.

## II. SPIN CHAINS

A variety of quantum spin chains exhibit quantum phase transitions. Therefore we begin with the study of a linear chain of spins with nearest neighbor interactions and open boundary conditions described by the Hamiltonian

$$H_{\text{chain}} = B \sum_{i=1}^N \sigma_i^z + \sum_{i=1}^{N-1} (J_x \sigma_i^x \sigma_{i+1}^x + J_y \sigma_i^y \sigma_{i+1}^y + J_z \sigma_i^z \sigma_{i+1}^z). \quad (1)$$

Here  $N$  is the number of spins,  $B$  a magnetic field and  $J_x$ ,  $J_y$  and  $J_z$  the interaction between neighboring spins. Two ancilla systems (named  $S$  for “sender” and  $R$  for “receiver”) couple to the chain at spins  $m_S$  and  $m_R$ , which are near the center of the chain in order to avoid boundary effects. The total Hamiltonian of chain and ancillas then reads

$$H = H_{\text{chain}} + B_a (\sigma_S^z + \sigma_R^z) + J_a (\sigma_S^x \sigma_{m_S}^x + \sigma_R^x \sigma_{m_R}^x), \quad (2)$$

where  $B_a \geq 0$  is the Zeeman splitting of the ancillas, which might differ from  $B$ , and  $J_a \geq 0$  the coupling of the ancillas to the chain, which is taken to be weak, i.e.  $J_a \ll (B, J_x, J_y, J_z)$ . As an initial state of the system we consider

$$|\Psi(0)\rangle = |\uparrow_S, \downarrow_R, 0_{\text{chain}}\rangle, \quad (3)$$

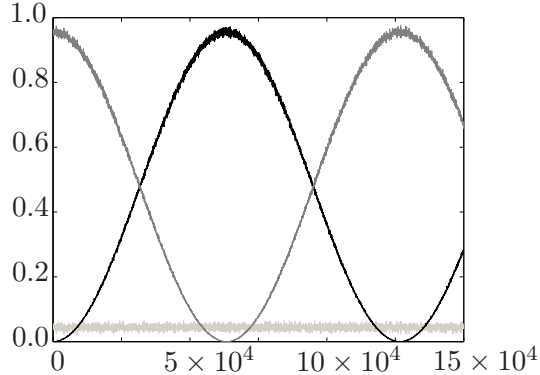


FIG. 1:  $P(\downarrow_S\downarrow_R)(t)$  (light gray),  $P(\uparrow_S\downarrow_R)(t)$  (gray) and  $P(\downarrow_S\uparrow_R)(t)$  (black) for  $B = 1$ ,  $J_x = 0.3$ ,  $J_y = J_z = 0$ ,  $B_a = 0.64$  and  $J_a = 0.05$  as given by the simulation for the open boundary model with  $N = 100$  spins.  $S$  couples to spin 45 and  $R$  to spin 55. Figure taken from [13].

i.e. the sender is spin up and the receiver is spin down, while the chain is in its ground state,  $|0_{\text{chain}}\rangle$ . This will allow us to explore the propagation of this excitation through the chain.

The dynamics is simulated with a matrix product state technique using matrices of dimension  $10 \times 10$  [14, 16]. The accuracy of the simulations was confirmed by varying the matrix dimension and the size of the time steps. Furthermore, we confirmed that the dynamics conserves the total energy of the system.

Figure 1 shows the probability  $P(\uparrow_S\downarrow_R)$  that “sender”  $S$  is in its excited state  $|\uparrow_S\rangle$  and the “receiver”  $R$  in its ground state  $|\downarrow_R\rangle$ , together with  $P(\downarrow_S\uparrow_R)$  and  $P(\downarrow_S\downarrow_R)$  for a model with  $N = 100$ ,  $m_S = 45$ ,  $m_R = 55$ ,  $B = 1$ ,  $J_x = 0.3$ ,  $J_y = J_z = 0$ ,  $B_a = 0.64$  and  $J_a = 0.05$ .  $P(\uparrow_S\uparrow_R)$  is always less than  $10^{-4}$ . The plots show that the excitation that was initially located in  $S$  oscillates back and forth between  $S$  and  $R$ .

Figure 2 shows  $P(\uparrow_S\downarrow_R)$ ,  $P(\downarrow_S\uparrow_R)$  and  $P(\downarrow_S\downarrow_R)$  for a model with  $N = 600$ ,  $m_S = 295$ ,  $m_R = 305$ ,  $B = 1$ ,  $J_x = 0.3$ ,  $J_y = J_z = 0$ ,  $B_a = 0.8$  and  $J_a = 0.05$ . Again,  $P(\uparrow_S\uparrow_R)$  is always less than  $10^{-4}$ . For these parameters, the excitation is not fully transferred to  $R$ , contrary to figure 1. Both,  $S$  and  $R$  relax to their ground states with the excitation only being partially and temporarily transferred to  $R$ , even for close-lying spins. Note that the parameters chosen in figures 1 and 2 are the same except for  $B_a$  which in figure 2 is significantly larger than in figure 1.

The two observed scenarios are rather generic. To demonstrate this, we have done the same simulations for a XXZ-model. The results, shown in figures 3 and 4, clearly agree with

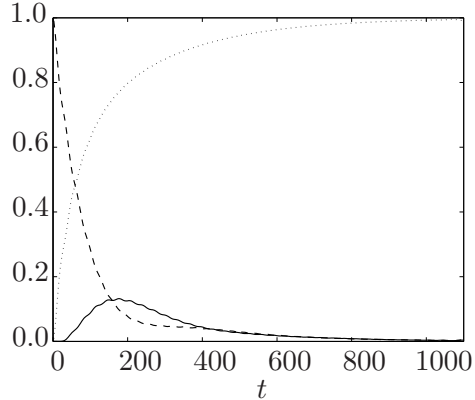


FIG. 2:  $P(\downarrow_S \downarrow_R)(t)$  (dotted line),  $P(\uparrow_S \downarrow_R)(t)$  (dashed line) and  $P(\downarrow_S \uparrow_R)(t)$  (solid line) for  $B = 1$ ,  $J_x = 0.3$ ,  $J_y = J_z = 0$ ,  $B_a = 0.8$  and  $J_a = 0.05$  as given by the simulation for the open boundary model with  $N = 600$  spins.  $S$  couples to spin 295 and  $R$  to spin 305. Figure taken from [13].

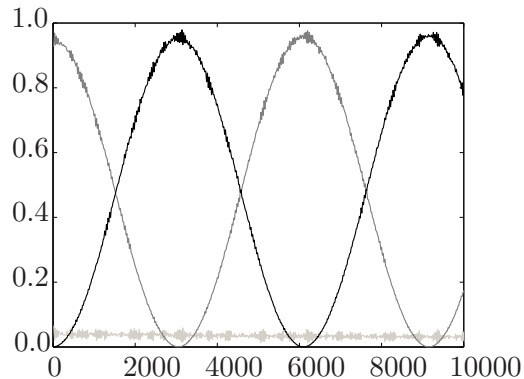


FIG. 3:  $P(\downarrow_S \downarrow_R)(t)$  (light gray),  $P(\uparrow_S \downarrow_R)(t)$  (gray) and  $P(\downarrow_S \uparrow_R)(t)$  (black) for  $B = 1$ ,  $J_x = 0.5$ ,  $J_y = 0.2$ ,  $J_z = 0.1$ ,  $B_a = 0.04$  and  $J_a = 0.05$  as given by the simulation for the open boundary model with  $N = 100$  spins.  $S$  couples to spin 45 and  $R$  to spin 55. Figure taken from [13].

our findings for the previous coupling parameters. Again  $B_a$  in figure 4 is significantly larger than in figure 3, while all other parameters are equal.

### III. SIMPLIFIED PHYSICAL PICTURE

The exact dynamics of a quantum spin chain is extraordinarily complex. Nevertheless, underlying the dramatic difference between the almost perfect transfer scenarios in figures 1 and 3 and the damped scenario in figures 2 and 4 is a simple physical mechanism. The

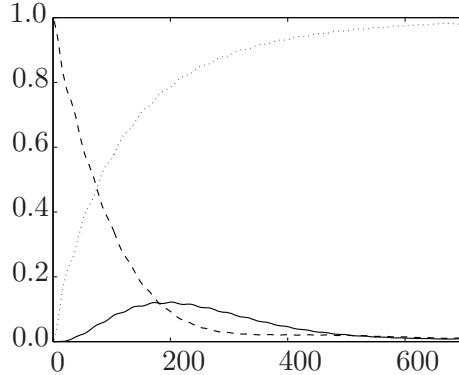


FIG. 4:  $P(\downarrow_S \downarrow_R)(t)$  (dotted line),  $P(\uparrow_S \downarrow_R)(t)$  (dashed line) and  $P(\downarrow_S \uparrow_R)(t)$  (solid line) for  $B = 1$ ,  $J_x = 0.3$ ,  $J_y = 0.2$ ,  $J_z = 0.1$ ,  $B_a = 0.2$  and  $J_a = 0.05$  as given by the simulation for the open boundary model with  $N = 600$  spins.  $S$  couples to spin 295 and  $R$  to spin 305. Figure taken from [13].

dynamics we have simulated is given by the Schrödinger equation containing the Hamiltonian (2). As a consequence, all moments of the Hamiltonian are conserved. The initial state  $|\Psi(0)\rangle$ , where one of the ancillas is excited, is not an eigenstate of  $H$  as given by (2). The mean value is  $\langle \Psi(0) | H | \Psi(0) \rangle$  and the variance of the energy is given by

$$\Delta E = \sqrt{\langle \Psi(0) | H^2 | \Psi(0) \rangle - \langle \Psi(0) | H | \Psi(0) \rangle^2} = \sqrt{2} J_a. \quad (4)$$

Given that the evolution is assumed to be Hamiltonian, both are in fact time invariant. Thus in the entire dynamics only those states with an energy expectation value  $\bar{E}$  in the range  $\langle \Psi(0) | H | \Psi(0) \rangle - \sqrt{2} J_a < \bar{E} < \langle \Psi(0) | H | \Psi(0) \rangle + \sqrt{2} J_a$  play a significant role as indicated by Figure 5.  $S$  and  $R$  are depicted as two level systems, while for the chain there is a unique ground state and a quasi continuous band of excited states sketched as the gray area. The dots indicate the initial occupations. The relevant energy range given by the variance lies between the two horizontal dashed lines. If the spectral gap is larger than the Zeeman splitting of the ancillas (left plot) it is not possible to create a real excitation of the chain, only processes involving virtual excitations of the chain are then permitted and the excitation will be almost completely transferred from  $S$  to  $R$ . If however the spectral gap is smaller than the Zeeman splitting of the ancillas, real excitations may be created in the chain. These excitations dephase rapidly due to the large number of accessible energy levels which prevents their reabsorption – the chain acts as a bath and information is lost.

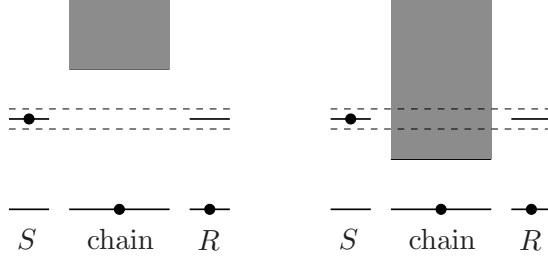


FIG. 5: Sketch of the energy levels of the system. The dots indicate the occupations of the initial state. For this initial state only the energy levels between the two horizontal dashed lines are accessible, resulting in almost perfect transfer for the left scenario and damping for the right one.

We believe that this heuristic picture captures the essential physics. To further corroborate our simple physical model and to underline the generality of our findings, we now turn to a different model for the chain which also features an adjustable energy gap above its unique ground state.

#### IV. HARMONIC CHAIN

Harmonic chains whose time evolution is governed by a Hamiltonian that is quadratic in position and momentum can be solved exactly in a compact form and therefore lend themselves to analytical investigations. Furthermore, Gaussian initial states, ie states whose Wigner function is a Gaussian, preserve their Gaussian character under the time evolution. As a Gaussian is fully described by its first and second moments this allows for a very compact, polynomial in the number of oscillators, description of the state of the systems and its evolution in time (see e.g. [19] for details), which permits the numerical investigation of very large systems. This is the basic motivation for the study of harmonic systems in Gaussian states in this section.

We consider a harmonic chain with periodic boundary conditions described by

$$H_{\text{chain}} = \frac{1}{2} \sum_{j=1}^N (p_j^2 + \Omega^2(q_j - q_{j+1})^2 + \Omega_0^2 q_j^2) \quad (5)$$

with the  $p_j$  being the momenta and the  $q_j$  the positions ( $q_{N+1} = q_1$ ). In this case, the two ancillas are harmonic oscillators that couple to oscillators  $m_S$  and  $m_R$  of the chain. The

complete Hamiltonian reads

$$H_{\text{tot}} = H_{\text{chain}} + H_{\text{ancillas}} + H_I \quad (6)$$

$$H_{\text{ancillas}} = \frac{1}{2} (p_S^2 + \omega^2 q_S^2 + p_R^2 + \omega^2 q_R^2) \quad (7)$$

$$H_I = J_a (q_S q_{m_S} + q_R q_{m_R}). \quad (8)$$

We are interested in the time evolution of the ancillas only. Thus, we will now derive an approximate master equation for the reduced density matrix  $\sigma(t)$  of the two ancilla systems.

For weak coupling  $J_a \ll (\Omega, \Omega_0)$  we find

$$\frac{d\sigma}{dt} = - \int_0^t ds \text{Tr}_{\text{chain}} \{ [H_I(t), [H_I(s), |0\rangle\langle 0| \otimes \sigma(s)]] \}, \quad (9)$$

where  $\sigma(t)$  is the reduced density matrix of the ancillas,  $\text{Tr}_{\text{chain}}$  is the trace over the degrees of freedom of the chain and  $|0\rangle$  denotes the ground state of the chain (5).  $H_I(t)$  is the interaction between ancillas and chain in the interaction picture. Here  $H = H_0 + H_I$  with  $H_0 = H_{\text{chain}} + H_{\text{ancillas}}$  and

$$H_I(t) = e^{iH_0 t} H_I e^{-iH_0 t}$$

and

$$\sigma(t) = e^{iH_0 t} \rho e^{-iH_0 t}.$$

Eq. (9) is an expansion in the coupling strength  $J_a$  up to second order, which is a good approximation if the integral approaches a constant value for  $t > t^*$ , where  $J_a t^* \ll 1$ . Since  $\sigma$  only changes significantly on time scales  $t \sim J_a^{-1} \gg t^*$ , the approximation  $\sigma(s) \approx \sigma(t)$  can be used. Performing the trace on the rhs of (9) yields

$$\begin{aligned} \frac{d\sigma}{dt} = -J_a^2 \sum_{j,l=S,R} & \left( -i (Y_1 + (Y_0 - Y_1)\delta_{jl}) [a_j a_l^\dagger, \sigma] \right. \\ & \left. + (X_1 + (X_0 - X_1)\delta_{jl}) \left( \{a_j a_l^\dagger, \sigma\} - 2(a_j \sigma a_l^\dagger) \right) \right), \end{aligned} \quad (10)$$

where  $[\cdot, \cdot]$  and  $\{\cdot, \cdot\}$  denote commutators and anti-commutators and  $a_S$  and  $a_R$  are the annihilation operators of  $S$  and  $R$ , respectively

$$\begin{aligned} q_j &= \frac{1}{\sqrt{2\omega}} (a_j + a_j^\dagger) \\ p_j &= -i\sqrt{\frac{\omega}{2}} (a_j - a_j^\dagger) \end{aligned}$$



for  $j = S, R$ . In deriving (10), we applied a rotating wave approximation. The coefficients read

$$\begin{aligned} X_0 &= \frac{1}{2\omega} \text{Re}(C_{m_S m_S}^+ + C_{m_S m_S}^-), \\ X_1 &= \frac{1}{2\omega} \text{Re}(C_{m_S m_R}^+ + C_{m_S m_R}^-), \\ Y_0 &= \frac{1}{2\omega} \text{Im}(C_{m_S m_S}^+ + C_{m_S m_S}^-), \\ Y_1 &= \frac{1}{2\omega} \text{Im}(C_{m_S m_R}^+ + C_{m_S m_R}^-) \end{aligned}$$

with  $C_{kl}^\pm$  given by

$$C_{kl}^\pm(t) = \int_0^t ds \langle 0|q_k(t)q_l(s)|0\rangle e^{\pm i\omega(t-s)}, \quad (11)$$

where  $k, l = m_S, m_R$ . Due to the symmetries of the model, we have  $C_{m_S m_S}^\pm = C_{m_R m_R}^\pm$  and  $C_{m_S m_R}^\pm = C_{m_R m_S}^\pm$ . Eq. (10) is a good approximation whenever  $C_{kl}^\pm(t) \approx \overline{C}_{kl}^\pm = \text{const.}$  for  $t \ll J_a^{-1}$ . Since the  $C_{kl}^\pm(t)$  do not depend on  $J_a$  themselves, there is always a sufficiently small  $J_a$  such that this holds, provided  $\lim_{t \rightarrow \infty} C_{kl}^\pm(t)$  exists. The validity of the master equation can be confirmed by a numerical simulation for a chain with 1400 oscillators. We found good agreement between our analytical and numerical solutions, with the relative errors being less than 5%.

The harmonic chain can be diagonalized via a Fourier transform [2]. In the limit of an infinitely long chain,  $N \rightarrow \infty$ , the correlation functions read

$$\langle 0|q_j(t)q_l(s)|0\rangle = \frac{1}{2\pi} \int_0^\pi dk \frac{1}{\omega_k} \cos((j-l)k) e^{-i\omega_k(t-s)}, \quad (12)$$

where  $\omega_k^2 = 4\Omega^2 \sin^2(k/2) + \Omega_0^2$  with  $-\pi < k < \pi$ . and all  $\lim_{t \rightarrow \infty} C_{kl}^\pm(t)$  exist except for the case where  $\omega = \Omega_0 = 0$ . As in master equations for system bath models, we now insert the asymptotic expressions,  $\overline{C}_{kl}^\pm = \lim_{t \rightarrow \infty} C_{kl}^\pm(t)$ , into eq. (10). This replacement assumes that all internal dynamics of the chain happens on much shorter time scales than the dynamics caused by the interaction of the ancillas with the chain. Furthermore, it does not treat the initial evolution for short times with full accuracy since  $\lim_{t \rightarrow 0} C_{kl}^\pm(t) = 0 (\neq \overline{C}_{kl}^\pm)$ . The master equation thus obtained is therefore valid in a regime where the couplings  $J_a$  are weak enough such that the time it takes for an excitation to travel from  $S$  to  $R$  is completely determined by  $J_a$ , i.e. by the time it takes to be transferred into and from the chain.

From eq. (10) we find the following solution for the expectation values of the occupation

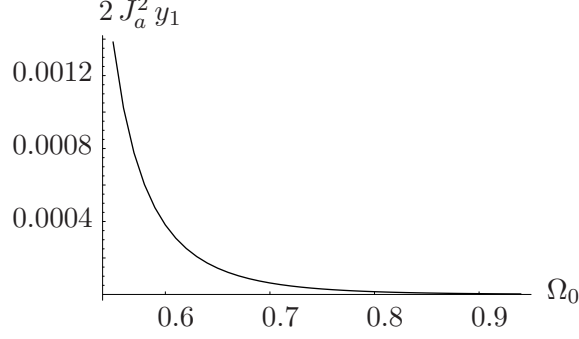


FIG. 6: Frequencies  $2J_a^2 y_1$  of the excitation's oscillation between  $S$  and  $R$  for  $\Omega = 1$ ,  $J_a = 0.05$  and  $\omega = 0.5$ . The transfer speed increases as  $\Omega_0 - \omega \rightarrow 0$ . Figure taken from [13].

numbers of  $S$  and  $R$ ,  $n_S = \text{Tr}(a_S^\dagger a_S \sigma)$  and  $n_R = \text{Tr}(a_R^\dagger a_R \sigma)$ :

$$\left. \begin{array}{l} n_S(t) \\ n_R(t) \end{array} \right\} = \left( \frac{n_S(0) + n_R(0)}{2} \cosh(2J_a^2 x_1 t) \pm \frac{n_S(0) - n_R(0)}{2} \cos(2J_a^2 y_1 t) \right) e^{-2J_a^2 x_0 t}. \quad (13)$$

Here,  $x_0 = \lim_{t \rightarrow \infty} X_0$ ,  $x_1 = \lim_{t \rightarrow \infty} X_1$  and  $y_1 = \lim_{t \rightarrow \infty} Y_1$ . Note that  $x_0 > 0$  and  $x_0 > |x_1|$ . Inserting the correlation functions into eq. (11) one sees that  $x_0$  and  $x_1$  are only non-zero if  $\omega \geq \omega_k$  for at least one mode  $k$ , that is if our initial state is in resonance with states where both ancillas are in their ground states and the chain is in one of its lowest-lying excited states (c.f. figure 5). The dispersion relation shows that this only happens for  $\omega \geq \Omega_0$ . As in figures 1 and 2 or 3 and 4, we thus observe two different scenarios:

If  $\omega < \Omega_0$ , and therefore  $x_0 = x_1 = 0$ , the excitation that is initially in  $S$  oscillates back and forth between  $S$  and  $R$  at a frequency  $2J_a^2 y_1$ , i.e.

$$\left. \begin{array}{l} n_S(t) \\ n_R(t) \end{array} \right\} = \frac{n_S(0) + n_R(0)}{2} \pm \frac{n_S(0) - n_R(0)}{2} \cos(2J_a^2 y_1 t). \quad (14)$$

Note in particular that the excitation is entirely transferred to  $R$  at times  $t_n = n(\pi/J_a^2 y_1)$ ;  $n = 1, 2, \dots$ . Figure 6 shows the frequencies  $2J_a^2 y_1$  of the excitation's oscillations between  $S$  and  $R$  for cases where  $\omega < \Omega_0$ , for  $\Omega = 1$ ,  $J_a = 0.05$  and  $\omega = 0.35$  as a function of  $\Omega_0$ . As  $\Omega_0 - \omega$  decreases, the transfer becomes faster and the oscillation frequency increases.

Let us examine the dependence of the oscillation frequency  $2J_a^2 y_1$  on the distance  $|m_S - m_R|$ . With the definitions of  $y_1$  and  $Y_1$  and eqs. (11), (12) and  $\int_0^\infty d\tau e^{-ix\tau} = \pi\delta(0) - i\mathcal{P}\frac{1}{x}$ ,

where  $\mathcal{P}$  denotes the principal value, we find

$$2J_a^2 y_1 = -\frac{J_a^2}{2\pi\omega} \int_{-\pi}^{\pi} dk \frac{\cos(|m_S - m_R|k)}{4\Omega^2 \sin^2(k/2) + \Omega_0^2 - \omega^2}. \quad (15)$$

Using the substitution  $z = e^{ik}$ , this integral can be converted to an integral over the unit circle, which in turn can be evaluated via the residue theorem [15]. The result is

$$2J_a^2 y_1 = -\frac{J_a^2}{8\omega\Omega^2} \frac{z^{|m_S - m_R|} + z^{-|m_S - m_R|}}{\sqrt{\alpha^2 + \alpha}} \quad (16)$$

where  $z = 2\sqrt{\alpha^2 + \alpha} - (2\alpha + 1)$  and  $\alpha = (\Omega_0^2 - \omega^2)/4\Omega^2$ . The frequency  $2J_a^2 y_1$  and hence the transfer speed decrease exponentially with increasing  $|m_S - m_R|$ .

If, on the other hand,  $\omega \geq \Omega_0$ , the chain acts similarly to a bath. Here,  $x_0 \neq 0$ ,  $x_1 \neq 0$ , and both ancillas relax into their ground state transferring their energy into the chain. During this process, however, a fraction of the energy initially located in  $S$  appears momentarily in  $R$  before it is finally damped into the chain. The maximal excitation of the receiver throughout the entire evolution depends on the distance  $|m_S - m_R|$ . For a given initial energy in  $S$ , only a narrow range of the excitation spectrum is relevant for the dynamics. Hence all relevant modes of the chain have very similar wavelength. If the distance  $|m_S - m_R|$  is a multiple of half that wavelength, a wave that has high amplitude next to  $S$  will have high amplitude next to  $R$ , too. In that case, the maximal excitation probability in  $R$  will be relatively large, although less than 0.5. If on the other hand, a wave that has high amplitude next to  $S$  has zero amplitude next to  $R$ , the transfer vanishes completely. Figure 7 shows the solution (13) for a harmonic chain and ancillas with  $\Omega = 1$ ,  $\omega = 0.5$ ,  $J_a = 0.05$ ,  $|m_S - m_R| = 9$  and  $\Omega_0 = 0.2$ . One might try to derive the same type of master equation for the spin chain (1). In the next section, we explain why such an approach is problematic when attempted with standard techniques.

### A. The problem of even and odd excitation number subspaces for spin chains

The standard procedure to diagonalize say the transverse Ising chain is a Jordan Wigner transformation followed by Fourier and Bogoliubov transformations [17]. This procedure however only diagonalizes the subspace of odd or even number of excitations at a time but not both. Since the operator  $\sigma_j^x$  maps between the odd to the even number subspaces for any  $j$ , an exact expression for the time dependent correlation functions  $\langle 0 | \sigma_j^x(t) \sigma_l^x(s) | 0 \rangle$ , which

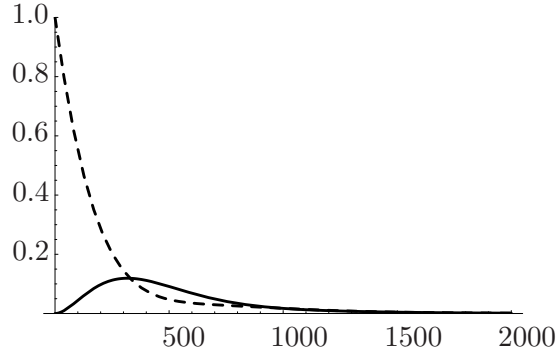


FIG. 7: The solution (13) for a harmonic chain and ancillas with  $\Omega = 1$ ,  $\omega = 0.5$ ,  $J_a = 0.05$ ,  $|m_S - m_R| = 9$  and  $\Omega_0 = 0.2$ . Figure taken from [13].

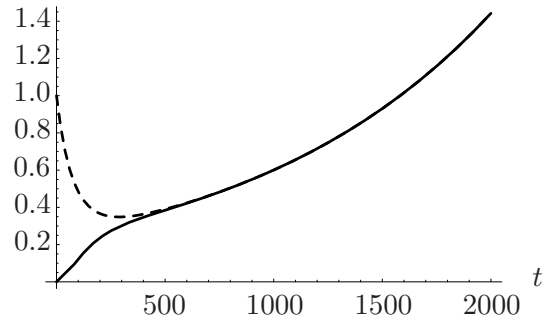


FIG. 8:  $P(\uparrow_S \downarrow_R)(t)$  (dashed line) and  $P(\downarrow_S \uparrow_R)(t)$  (solid line) for  $B = 1$ ,  $J_x = 0.3$ ,  $J_y = J_z = 0.0$ ,  $B_a = 0.8$  and  $J_a = 0.05$  as given by the solution of a master equation for the transverse Ising spin chain. The solution is not physical since probabilities are not less or equal to 1.

would be required for deriving a master equation, cannot be obtained via the above procedure [18]. If one uses only say the even excitation number subspace as an approximation, the errors for the obtained eigenvalues scale as  $1/N$ , where  $N$  is the length of the chain. It is therefore often argued that only using one subspace is a good approximation for long chains.

In our problem, this reasoning cannot be applied: An approximation of the required correlation functions,  $\langle 0 | \sigma_j^x(t) \sigma_l^x(s) | 0 \rangle$ , by only considering one subspace leads to unphysical results for the master equation. An example is given in figure 8. We have therefore avoided a treatment of the spin chains with master equations.

## V. CONCLUSIONS

Quantum spin chains may be used as quantum channels. Here we have studied the dependence of the transfer quality and speed on the size of the spectral gap between the ground and the lowest excited state of the considered system.

Two different scenarios are observed: Provided the spectral gap of the chain is larger than the amount of energy initially located in the sender, close to perfect transfer happens on rather long time scales. The transfer becomes even more perfect but slower if the coupling strength between ancillas and chain or the energy initially in the sender is lowered further.

If the energy in the sender is initially larger than the spectral gap, the behavior changes significantly. Here, the excitations get lost into the chain implying a bad transfer quality. This second scenario takes place on much shorter time scales than the first one.

These results may be used for two main applications: For quantum information purposes, they show, that by using a system with a large enough spectral gap one can build good quantum channels. These channels are furthermore considerably robust against decoherence because the chain remains to a high precision in its ground state which is not significantly affected by an environment at zero temperature.

In condensed matter physics, on the other hand, the transfer speed and quality can be used to infer the size of the spectral gap and hence the location of quantum critical points. This method is admittedly inferior to neutron scattering in magnetic composites, but it may be advantageous in optical lattices where neutron scattering is not that successful.

### Acknowledgments

The authors would like to thank Sougato Bose and Daniel Burgarth for discussions at early stages of this project as well as comments by Andrew Fisher. This work is part of the QIP-IRC supported by EPSRC (GR/S82176/0), the Integrated Project Qubit Applications (QAP) supported by the IST directorate as Contract Number 015848' and was supported

also by the Alexander von Humboldt Foundation, Hewlett-Packard and the Royal Society.

---

- [1] Bose S. Phys. Rev. Lett. **91**, 207901 (2003).  
Burgarth D and Bose S. New J. Phys. **7**, 135 (2005).
- [2] Plenio M B, Hartley J, and Eisert J. New J. Phys. **6**, 36 (2004).  
Eisert J, Plenio M B, Bose S, and Hartley J. Phys. Rev. Lett. **93**, 190402 (2004).  
Plenio M B and Semião F. New J. Phys. **7**, 73 (2005).  
Perales A and Plenio M B J. Opt. B **7**, 601 (2005)
- [3] Hastings M B Phys. Rev. Lett. **93**, 126402 (2004).  
Hastings M B Phys. Rev. B **69**, 104431 (2004).  
Hastings M B Phys. Rev. B **73**, 085115 (2006).  
Hastings M B Phys. Rev. Lett. **93**, 140402 (2004).
- [4] Cramer M, Eisert J, Plenio M B and Dreissig J. Phys. Rev. A **73**, 012309 (2006).  
Cramer M and Eisert J. New J. Phys. **8**, 71 (2006).  
Wolf M M, Giedke G and Cirac J I. Phys. Rev. Lett. **96**, 080502 (2006).
- [5] Sachdev S *Quantum Phase Transitions*. Cambridge Univ. Press, Cambridge, (1999).
- [6] Osterloh A, Amico L, Falci G and Fazio R. Nature **416**, 608 (2002).
- [7] Verstraete F, Martín-Delgado M A and Cirac J I. Phys. Rev. Lett. **92**, 087201 (2004).  
Pachos J K and Plenio M B. Phys. Rev. Lett. **93**, 056402 (2004).  
Kay A, Lee D K K, Pachos J K, Plenio M B, Reuter M E and Rico E. Optics and Spectroscopy **99**, 339 - 356 (2005).
- [8] Larsson D and Johannesson H. Phys. Rev. Lett. **95**, 196406 (2005).
- [9] Amico L, Osterloh A, Plastina F, Fazio R and Massimo Palma G Phys. Rev. A **69**, 022304 (2004).  
Dür W, Hartmann L, Hein M, Lewenstein M and Briegel H-J Phys. Rev. Lett. **94**, 097203 (2005).  
Sen De A, Sen U, Ahufinger V, Briegel H-J, Sanpera A and Lewenstein M quant-ph/0507172 (2005).
- [10] Sen A, Sen U and Lewenstein M. Phys. Rev. A **72**, 052319 (2005).
- [11] Yi X X, Cui H T and Wang L C. quant-ph/0511026 (2005).

- [12] Zurek W H, Dorner U and Zoller P. Phys. Rev. Lett. **95**, 105701 (2005).  
Polkovnikov A. Phys. Rev. B **72**, 161201(R) (2005).  
Dziarmaga J. Phys. Rev. Lett. **95**, 245701 (2005)
- [13] Hartmann M J, Reuter M E, and Plenio M B. New J. Phys. **8**, 94 (2006).
- [14] Östlund S, Rommer S Phys. Rev. Lett. **75**, 3537-3540 (1995).  
Vidal G. Phys. Rev. Lett. **93**, 040502 (2004).  
Daley A J, Kollath C, Schollwöck U and Vidal G. J. Stat. Mech.: Theor. Exp., P04005 (2004).
- [15] We like to thank Andrew Fisher for bringing this point to our attention.
- [16] Plenio M B, Eisert J, Dreissig J, and Cramer M. Phys. Rev. Lett. **94**, 060503 (2005).
- [17] Lieb E, Schultz T and Mattis D. Ann. Phys. **16**, 407 (1961).
- [18] McCoy B M. Phys. Rev. A **4**, 2331 (1971).
- [19] Eisert J. and Plenio M.B., Int. J. Quant. Inform. **1**, 479 (2003)